Analysis of neutron emission spectra for 30–50 MeV α-particle induced reactions in thick targets

D. Dhar
Department of Physics, Visva Bharati, Santiniketan 731235, India

S. N. Roy
Department of Physics, Visva Bharati, Santiniketan 731235, India

Maitreyee Nandy
Saha Institute of Nuclear Physics, 1/AF, Bidhannagar, Calcutta 700 064, India

P. K. Sarkar
H. P. Unit, Variable Energy Cyclotron Centre, 1/AF, Bidhannagar, Calcutta 700 064, India

(Received 30 January 2003; published 27 June 2003)

Comparisons of calculated neutron yield distributions from α-particle induced reactions on thick targets are made with measured data to analyze the initial reaction process in the framework of the exciton (hybrid) model code ALICE91 (M. Blann, Lawrence Livermore National Laboratory Report UCID 19614, 1982). We have considered two reaction mechanisms: dissolution of the α in the nuclear field, and preequilibrium processes initiated by α-nucleon collisions. Both these processes seem to contribute to the emitted neutron spectra in varying proportions depending on the incident α energy and possibly on the target nucleus. Contributions from other processes appear to be non-negligible.

DOI: 10.1103/PhysRevC.67.064611 PACS number(s): 24.10.−i, 29.30.Hs, 25.55.−e

I. INTRODUCTION

Nuclear reactions induced by α particles are more complicated compared to nucleon-induced reactions because of the presence of processes that compete with complete fusion to initiate the reaction. Even at low incident energies, i.e., about 10 MeV/nucleon, the break-up of the projectile in the nuclear field has been found [1] to contribute noticeably to the total cross section. In an earlier work, Grimes *et al.* [2] concluded that neutron emission from α-induced reactions can be attributed to the direct reaction mechanism. Subsequent measurements of inclusive charged particle spectra from α-induced reactions on several nuclei [1] indicated that five different mechanisms may be responsible for the experimentally observed results. These are

(a) Inelastic scattering of incident α particles by the target nucleus as a whole. This leads to excitation of collective states above the particle emission threshold [3].

(b) Pickup reactions—creation of ^{5}He or ^{5}Li, followed by a breakup to a kinematically correlated α particle plus a nucleon [4].

(c) Binary fragmentation of the α particle [5–7].

(d) Dissolution of the α particle into four nucleons in the nuclear field [8,9].

(e) Interaction of the α particle with individual nucleons of the target nucleus, leading to a preequilibrium (PEQ) cascade of α-nucleon scattering.

The last three processes are similar in that each leads to the destruction of the α particle and initiation of a PEQ cascade. Some authors consider the fourth and fifth mechanisms as the same process, and the third merely the special case of either. In our opinion, this may not be true, since calculated particle emission spectra are likely to differ for each of these reaction mechanisms.

In the present work, we ignore the first two mechanisms as these together comprise about 5% of α particle-target nucleus interactions [10]. Further, in our analysis, we have also ignored the third mechanism which leads to emission of a fragment of the α at forward angles. We have considered only the last two reaction mechanisms that are major contributors to the total reaction cross section, and they lead to two different initial exciton configurations as described in the following. Our objective is to find out how important these two mechanisms are, and in what way, while calculating neutron emission spectra from α-induced reactions on thick targets. For our calculations we have selected the exciton (hybrid) model code ALICE91 [11] since in our earlier study [12] we have found that this code performs better than other exciton model codes in approximating α-particle-induced neutron emissions from thick targets. In the following section we give a brief outline of our theoretical calculations followed by results and discussions in Sec. III.

II. THEORETICAL CALCULATIONS

To study the α-particle-induced reactions in thick targets at low and intermediate energies, we have calculated the emitted neutron yield from $\alpha+^{27}$Al and $\alpha+^{48}$Ti reactions at 30, 40, and 50 MeV projectile energies at three different laboratory angles. The calculations have been performed using the exciton (hybrid)+Weisskopf-Ewing (WE) code ALICE91. We have compared the calculated results with our measured data at laboratory angles of 0°, 30°, and 45° [12]. In our region of interest, namely, 30–50 MeV α-induced reactions, we have assumed that the α particle interacts with the target nuclei in two principal modes:

(i) The α particle breaks into its four constituents and initiates the reaction process with a configuration of four

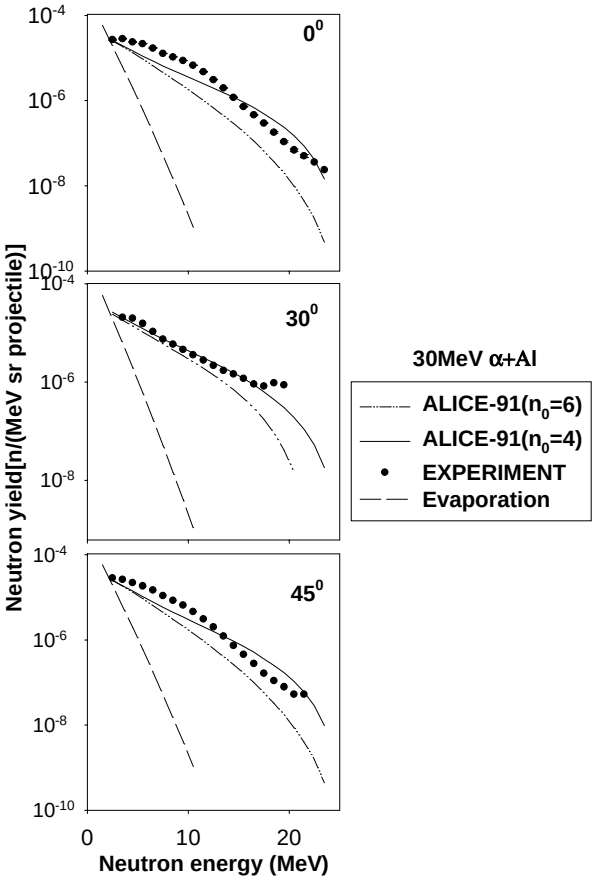

FIG. 1. Neutron yield distributions at 0°, 30°, and 45° for 30-MeV α particles bombarding thick Al targets. Measured data (solid circles) are compared with calculated results from ALICE91 code for $n_0=4$ (solid line) and $n_0=6$ (dot-dash line). Dashed lines are evaporation components calculated using $n_0=4$. Error bars in the experimental data are shown when they exceed the symbol size.

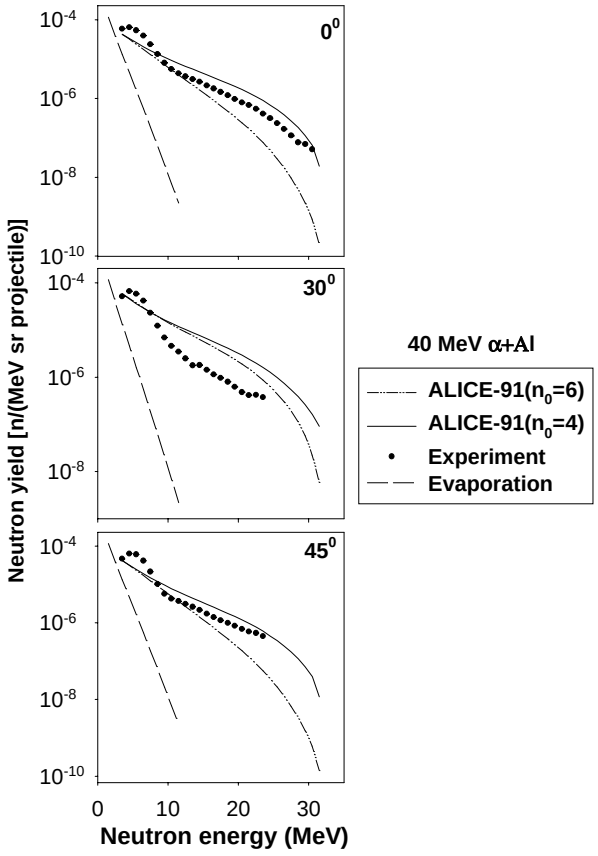

FIG. 2. Same as Fig. 1, but for 40 MeV incident α energy.

particles and zero hole $(4p0h)$. This is the reaction mechanism [case (d)] as described earlier.

(ii) The α projectile interacts with a target nucleon and lifts it above the Fermi sea to form the composite system giving an initial configuration of five particles and one hole $(5p1h)$ to start the relaxation process. This corresponds to the reaction mechanism [case (e)] as described earlier.

Thus our analysis of the observed neutron spectra using the exciton (hybrid) model leads to calculation of emission spectra from two different initial configurations, namely, $4p0h$ and $5p1h$. We have chosen our targets thick enough so that the projectiles are completely stopped inside them. The emitted neutron spectrum from any such thick target is in reality a sum of all the spectra from continuously degrading projectile energies, starting from the incident energy down to the threshold energy for neutron emission from the target nucleus. The code ALICE91 has been modified to take into account of this aspect. The details of the experiment and the modifications made in the code can be found in our earlier publication [12].

A. ALICE

In the framework of the hybrid model, each stage of relaxation of the target+projectile composite system towards equilibrium is described by the number n of excitons (excited particles and holes) in it [13]. The energy distribution of the ejectile at each exciton state is calculated explicitly from the phase space available to the ejectile. The total energy differential PEQ cross section for the ejectile is determined by summing over all exciton states starting from the initial state n_0. The PEQ energy spectrum is given by

$$\sigma_{PEQ}(\epsilon_x) = \sigma_{abs}(E_\alpha) \sum_{\substack{n=n_0 \\ \Delta n=2}}^{\bar{n}} D_n \left[{}_nX_x \frac{\rho_n(U,\epsilon_x)}{\rho_n(E_c)} \right] \frac{\lambda_c(\epsilon_x)}{\lambda_c(\epsilon_x)+\lambda_+(\epsilon_x)}, \tag{1}$$

where $\sigma_{abs}(E_\alpha)$ is the absorption cross section of the α projectile in the target at incident energy E_α. It is calculated using the parabolic model routine [11]. The other symbols have their usual meanings as explained in Ref. [12].

The lower limit n_0 of summation in Eq. (1) is the number of excitons in the initial stage. The value of this lower limit is taken as 4 or 6 depending, respectively, on the initial configuration $4p0h$ or $5p1h$ to be used. The upper limit $\bar{n}$ is the number of excitons when equilibrium is reached, and is given by

$$\bar{n}=(2gE_c)^{1/2}, \tag{2}$$

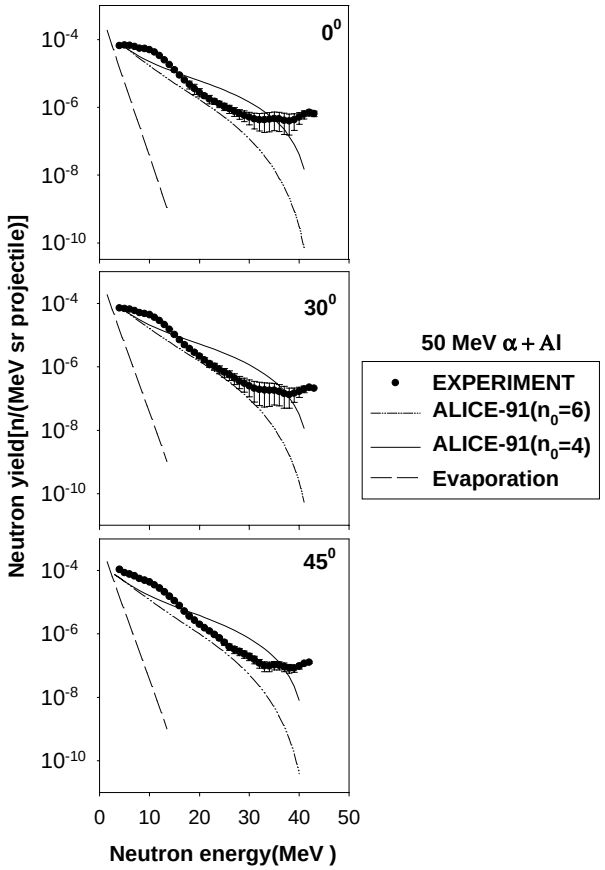

FIG. 3. Same as Fig. 1, but for 50 MeV incident α energy.

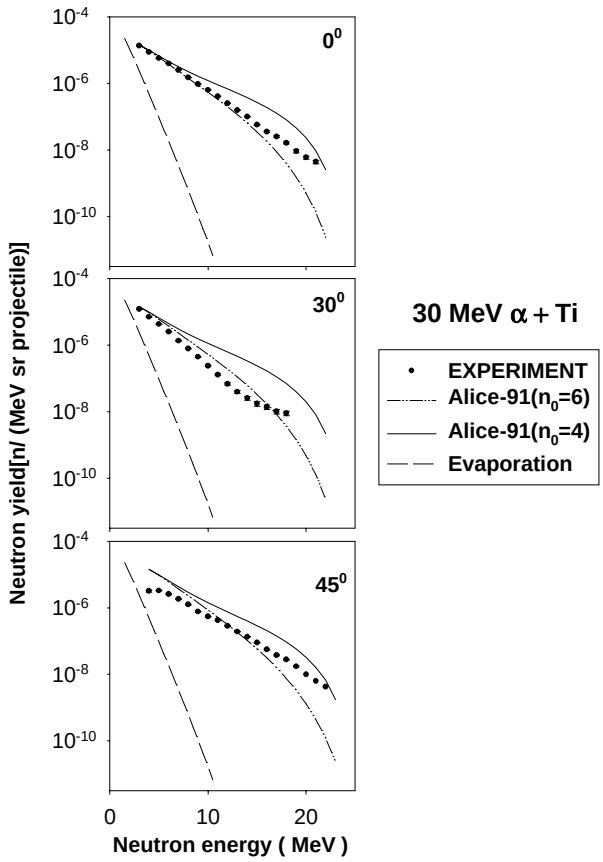

FIG. 4. Neutron yield distributions at 0°, 30°, and 45° for 30-MeV α particles bombarding thick Ti targets. Measured data (solid circles) are compared with calculated results from ALICE91 code for $n_0=4$ (solid line) and $n_0=6$ (dot-dash line). Dashed lines are evaporation components calculated using $n_0=4$. Error bars in the experimental data are shown when they exceed the symbol size.

where E_c is the total excitation energy of the composite system.

The evaporation or equilibrium (EQ) emission cross section is given by

$$\sigma_{EQ}(\epsilon_x) \sim \frac{e^{2(aU_r)^{1/2}}}{U_r}, \tag{3}$$

where a is the level density parameter ($=A/9$, A is the mass number of the residual nucleus) and U_r is the available excitation energy of the residual nucleus after EQ emissions. We have used the free Fermi gas level density option in ALICE91.

From the energy spectra the angular distribution for a x-type particle is calculated using Kalbach-Mann [14] systematics for PEQ emissions and isotropic distributions for the EQ emissions.

In its present form the code ALICE91 calculates PEQ emission of nucleons using the hybrid model followed by EQ emission of protons, neutrons, α particles, and deuterons using the WE formalism. Single and simultaneous two-nucleon PEQ emissions are considered, but there is no provision to calculate PEQ emission of clusters.

III. RESULTS AND DISCUSSIONS

In this work we have calculated (using the modified code ALICE91) double-differential neutron yield from α-induced reactions on thick targets of ^{27}Al and ^{48}Ti, and have compared with the measured data at 30 MeV, 40 MeV, and 50 MeV projectile energies. Calculations have been done separately for two different initial configurations, e.g., $4p0h$ ($n_0=4$) and $5p1h$ ($n_0=6$), to consider the two different reaction mechanisms for absorption of α particles in the target nucleus. The angular distribution of neutrons at laboratory angles 0°, 30°, and 45° at 30, 40, and 50 MeV incident α energies are plotted for $\alpha+^{27}$Al reactions in Figs. 1–3 and for $\alpha+^{48}$Ti reactions in Figs. 4–6. The total contributions from PEQ and EQ emissions are shown for $n_0=4$ (solid line) and $n_0=6$ (dot-dash line). The experimental data are plotted as solid circles (with error bars only when the error exceeds the symbol size). The EQ contribution for $n_0=4$ is also shown separately as long dashed lines. The EQ contribution for $n_0=6$ is not plotted since in this case the small increase compared to $n_0=4$ is not discernable.

It is seen from all the figures that, for the range of emission energies considered, evaporation contribution to neutron emission is restricted only to low energy part of the spectrum and is negligible above 5 MeV neutron emission energy. Calculated results with $n_0=6$ show lower neutron yield compared to those with $n_0=4$. The difference increases with

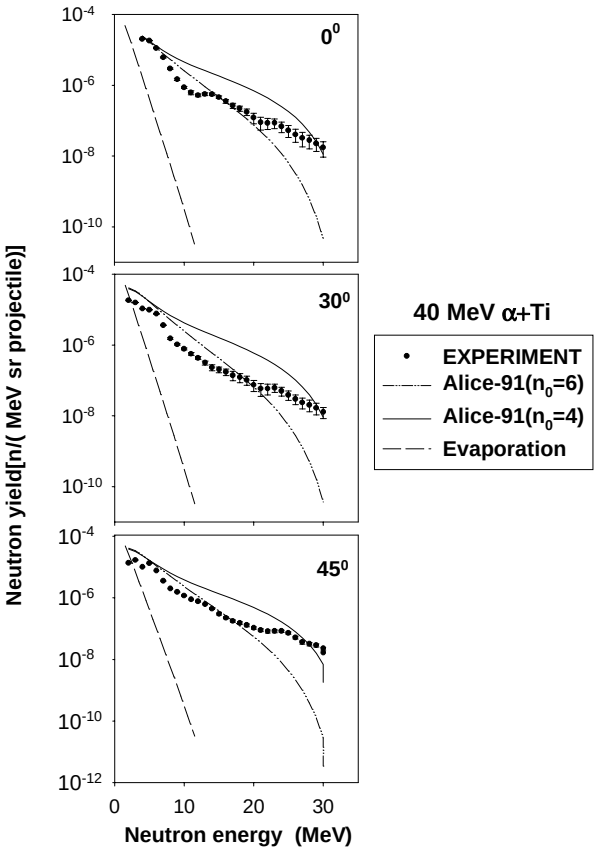

FIG. 5. Same as Fig. 4, but for 40 MeV incident α energy.

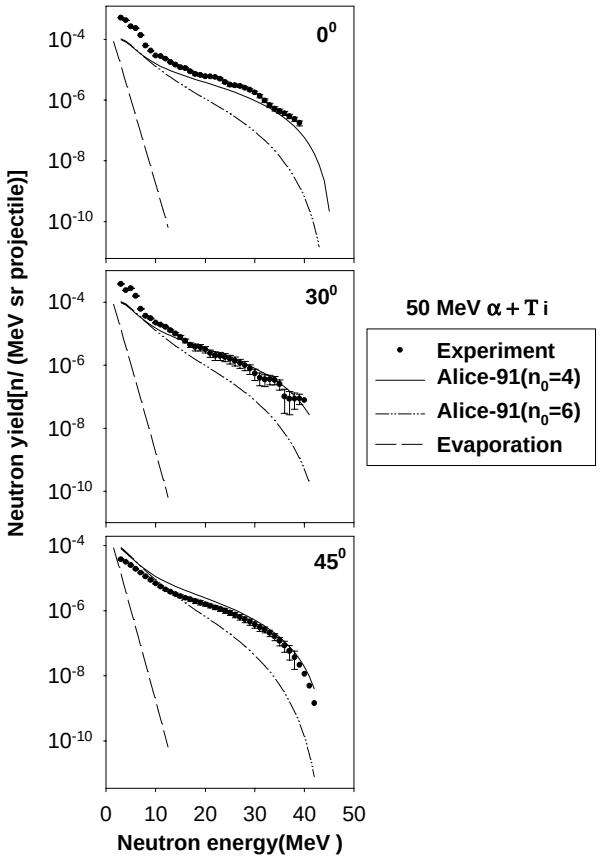

FIG. 6. Same as Fig. 4, but for 50 MeV incident α energy.

increasing neutron emission energy. This is understandable since, for ALICE91, $n_0=4$ configuration will have additional contribution of emitted neutrons from the $4p0h$ state compared to the $n_0=6$ configuration, which starts from $5p1h$ state. This additional contribution will predominantly be high energy neutrons because in the case of $n_0=4$ configuration the total excitation energy is shared among four excitons in contrast to $n_0=6$ configuration where the total excitation energy is shared among six excitons. This calculated difference between the two configurations is likely to be model dependent. Since ALICE91 works with a ''never come back'' assumption, it is not possible to reach a lower configuration state from a higher one (i.e., $4p0h$ from $5p1h$). This assumption is questionable, certainly at higher exciton configurations but not at the initial stages where ''coming back'' might occur with very low probability (if at all, for $5p1h$ to $4p0h$).

We also observe from the figures that the angular dependence of the emitted neutrons follows more or less the same trend as predicted by the Kalbach [14] systematics. This is concluded from the fact that though the overall agreement between calculated results and measured data is not good, the observed differences between the two distributions do not change with angle for a particular incident α energy.

At an incident energy of 30 MeV, the measured neutron distributions at the three angles have closer agreement with $n_0=4$ calculations, but not with those from $n_0=6$, which underpredict the measured data. But as the projectile energy increases, the intermediate and high energy part of the measured neutron emission data moves closer to $n_0=6$ results (Figs. 2 and 3). A combination of the two results in appropriate proportions is likely to reproduce the measured data more closely at all incident energies. However, the relative contribution from each mechanism seems to vary with incident α energy. It appears that with increasing incident α energy the contribution from $n_0=4$ is decreasing. This may be explained as follows. The dissolution of the α particle to four nucleons $(4p0h)$ in the nuclear field occurs most likely at the nuclear surface. The probability of occurrence of this mechanism can be assumed to be proportional to the product of the gradient of the nuclear potential and the interaction time of the α with the nucleus. The nuclear potential is relatively independent of the α energy. The interaction time, however, is inversely proportional to the velocity of the α and therefore proportional to $E_\alpha^{-1/2}$, roughly in keeping with the observed decrease.

This explanation, however, is not valid for the Ti target where the trend with increasing α energy is reverse. We can see that at 30 MeV incident α energy (Fig. 4), the measured data are better reproduced by $n_0=6$ calculations compared to $n_0=4$ results. On the other hand, in the case of 50 MeV incident αs the $n_0=4$ calculations estimate the measured data more closely. This trend is, however, consistent with the analysis of Grimes *et al.* [2] where with increasing α energy neutron emissions (attributed to direct reactions) are, in fact, emissions from the $n_0=4$ state.

Furthermore, we observe a ''shoulder'' in the emitted neu-

tron spectrum around 10 MeV for both the targets. This becomes prominent with increasing α energy. It is likely that these neutrons are contributed by the binary fragmentation of the α projectile, which we have ignored in our calculations. There are three possible modes of the binary fragmentation of the α, namely, $n+{}^3\mathrm{He}$, $p+t$, and $d+d$. The energy distribution of the fragments are approximately Gaussian in shape, with a mean centered about an energy corresponding to the beam velocity. One of the fragments may be moving in the forward direction and the complimentary one may be absorbed in the nucleus. Emission of neutrons directly from the binary fragmentation along with those from the secondary reactions initiated by the fragments may be the source of neutrons in the shoulder region. The estimated contribution from this process to the total reaction cross section is about 10% [1]. For thick targets the interaction probability of these binary fragments with the target nuclei is expected to be more compared to thin targets.

Another possible (though may occur with low probability) reaction mechanism that we have ignored is the neutrons emitted from the breakup of ${}^5\mathrm{He}$ formed in pickup reactions [mechanism (b) as described in the beginning]. The pickup of a neutron by the α projectile to form ${}^5\mathrm{He}$ and the subsequent breakup to $n+\alpha$ accounts for only about 2% of all events [1] (the relative percentage contribution for neutron emitting events may be a little higher). However, these neutrons might also contribute to the shoulder region of the energy distribution.

In our present calculations, we could not consider these processes in the framework of the hybrid model code that we have selected. We have to ignore the reactions induced by the secondary particles since our calculation is just a summation of thin target spectra at different decreasing incident energies. A detailed Monte Carlo tracking is necessary to take account of the reactions induced by secondary particles and projectile fragments.

IV. CONCLUSIONS

We have calculated neutron yield distributions from α-particle-induced nuclear reactions in thick targets of Al and Ti using the exciton (hybrid) model for PEQ emissions. We have compared the calculated results with our earlier measured data at incident energies of 30, 40, and 50 MeV. The calculations have been performed for two different absorption mechanisms leading to two different initial configurations $4p0h$ $(n_0=4)$ and $5p1h$ $(n_0=6)$. We have found that, in an overall situation, the measured distributions can be approximated more closely by a proportionate combination of both the configurations than by any one of them. The proportion in which they need to be combined depends on the incident α energy and possibly on the target mass. However, there are significant discrepancies between the observed data and the calculated results. These are likely to be due to reaction mechanisms that we have not considered in the present work. Thick target neutron yield data can be used to test the overall performance of a nuclear reaction model for a wide range of energies. The energy range starts from the incident projectile energy and goes down to the threshold energies for neutron emissions in different target nuclei. The limitations of simple exciton based models for estimating neutron emissions from α-induced reactions are apparent from the present study.

[1] E. Gadioli, E. Gadioli-Erba, J.J. Hogan, and B.V. Jacak, Phys. Rev. C **29**, 76 (1984).
[2] S.M. Grimes, J.D. Anderson, J.W. McClure, B.A. Pohl, and C. Wong, Phys. Rev. C **3**, 645 (1971).
[3] C. Mayer-Boricke, Nukleonika **22**, 1131 (1977).
[4] G. Chenevert, N.S. Chant, I. Halpern, G. Glashausser, and D.L. Hendrie, Phys. Rev. Lett. **27**, 434 (1971).
[5] R.W. Koontz, C.C. Chang, H.D. Holmgren, and J.R. Wu, Phys. Rev. Lett. **43**, 1862 (1979).
[6] J.R. Wu, R.W. Koontz, C.C. Chang, and H.D. Holmgren, Phys. Rev. C **20**, 1284 (1979).
[7] H. D. Holmgren, C. C. Chang, R. W. Koontz, and J. R. Wu, *Proceedings of the Second International Conference on Nuclear Reaction Mechanisms, Varenna, 1979*, (University of Milano, Milano, 1979).
[8] M. Blann, Annu. Rev. Nucl. Sci. **25**, 123 (1975), and references therein.
[9] E. Gadioli, Nukleonika **21**, 385 (1976), and references therein.
[10] E. Gadioli, and E. Gadioli-Erba, Z. Phys. A **299**, 1 (1981).
[11] M. Blann, Lawrence Livermore National Laboratory Report UCID 19614, 1982; Report No. SMR/284-1.
[12] D. Dhar, S.N. Roy, T. Bandyopadhyay, and P.K. Sarkar, Phys. Rev. C **67**, 024607 (2003).
[13] M. Blann, Phys. Rev. Lett. **27**, 337 (1971); **27**, 700(E) (1971); **28**, 757 (1972); Nucl. Phys. **A213**, 570 (1973).
[14] C. Kalbach and F. Mann, Phys. Rev. C **23**, 112 (1981); C. Kalbach, *ibid.* **25**, 3197 (1982).